HURRICANE FRED (2015)

Cape Verde's First Hurricane in Modern Times: Observations, Impacts, and Lessons Learned

Gregory S. Jenkins, Ester Brito, Emanuel Soares, Sen Chiao, Jose Pimenta Lima, Benvendo Tavares, Angelo Cardoso, Francisco Evora, and Maria Monteiro

Surface and satellite observations along with WRF Model forecasts provide a unique view of Hurricane Fred, the first to strike Cape Verde in 124 years.

Tropical cyclones remain the deadliest form of short- to medium-range weather hazards (Obasi 1994). While track forecasts have improved significantly, tropical cyclogenesis and rapid intensification remain challenges and have been the focus of recent field campaigns (Montgomery et al. 2012; Braun et al. 2013; Rogers et al. 2013). In the extreme eastern Atlantic, tropical cyclones are less frequent than in the central and western Atlantic because the waters are cooler and the Saharan air layer (SAL) can act as an inhibiting factor to development because of dry air, positive stability, and wind shear (Evan et al. 2006). However, dust associated with the SAL may also potentially lead to convective invigoration through microphysical processes (Koren et al. 2005; Jenkins et al. 2008; Rosenfeld et al. 2012). While infrequent, tropical depressions and storms have formed near the Cape Verde islands, as was the case during the NASA African Monsoon Multidisciplinary Analysis (NAMMA) campaign with Tropical Depression 8 and Tropical Storm (TS) Debby (Zipser et al. 2009; Zawislak and Zipser 2010).

Cape Verde is located approximately 400 miles (~644 km) to the west of Senegal. It comprises 10 islands, with significant variations in climate and landscape among the islands. These variations range from semiarid conditions in Sal and Boa Vista to wet conditions on the islands of Fogo, Santiago, and Brava. There are also variations in elevation, with mountains most prominent in the northwest on Santo Antão and São Nicolau and in the south on Fogo and Santiago (Fig. 1).

According to the results of the fourth population and housing census (2010), Cape Verde totals approximately 501,648 inhabitants, including residents and nonresidents, with a 1.2% annual-average growth from 2000 (434,625) to 2010 (491,575). Sotavento, consisting of the southern islands of Santiago, Brava, Fogo, and

AFFILIATIONS: Jenkins—Department of Meteorology, The Pennsylvania State University, University Park, Pennsylvania; Brito, Soares, Pimenta Lima, Tavares, Cardoso, Evora, and Monteiro—Institute for Meteorology and Geophysics, Ilha do Sal, Cape Verde; Chiao—Department of Meteorology and Climate Sciences, San Jose State University, San Jose, California
CORRESPONDING AUTHOR: Gregory S. Jenkins, gsj1@psu.edu

The abstract for this article can be found in this issue, following the table of contents.
DOI:10.1175/BAMS-D-16-0222.1

A supplement to this article is available online (10.1175/BAMS-D-16-0222.2)

In final form 10 April 2017

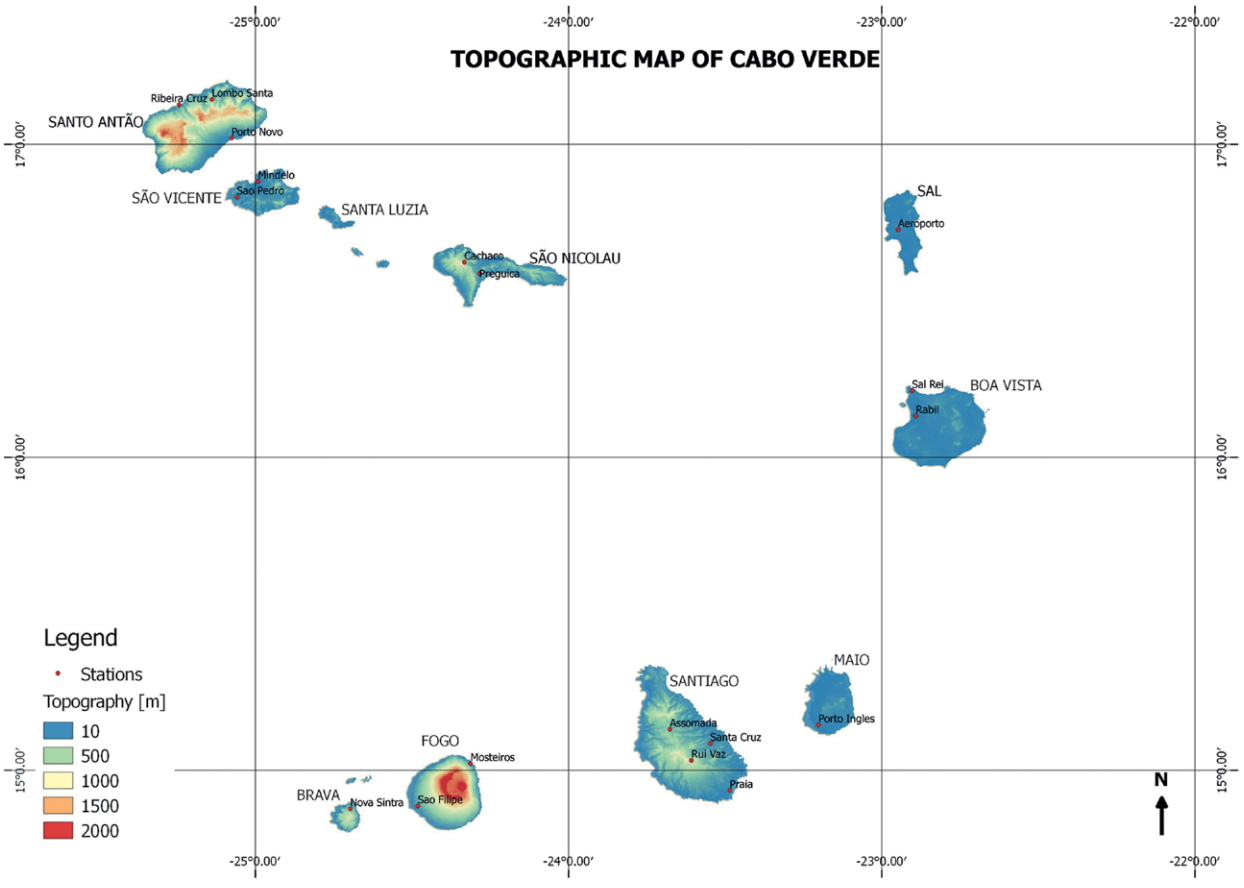

Fig. 1. The Cape Verde islands and their associated elevations (m).

Maio, is the most densely populated area, with approximately 323,917 inhabitants. Barlavento, consisting of the northern islands of Boa Vista, Sal, São Nicolau, Santa Luzia, São Vicente, and Santo Antão, has 127,658 inhabitants; Santa Luzia is uninhabited.

Cape Verde is a young, developing country (it became independent in 1975) that is very vulnerable to climate change and external factors since it imports approximately 90% of its consumption needs. Cape Verde suffers from a scarcity of natural resources, including drinking water, exacerbated by the long droughts and poor soil on several islands. The economy is service oriented, with commerce, transport, tourism, and public services accounting for about three-fourths of the gross domestic product (GDP). Although about 70% of the populations live in rural areas, agriculture and livestock are less developed and have a small contribution to the GDP; approximately 73% of foods have to be imported. The potential of the fishery sector, especially lobster and tuna fish, is not fully exploited. Tourism and salt exploitation are other important sources of revenue, contributing more than 10% of Cape Verde's $900 million GDP in 2005 (INE-CV 2011).

Most of the eastern Atlantic hurricanes form from African easterly waves (AEWs) when ocean temperatures are warm enough to support their formation. This occurs from mid-August through late September, when the African easterly jet (AEJ) and intertropical convergence zone (ITCZ) have the greatest northward extension and there is strong convection during the mature phase of the monsoon period (Zawislak and Zipser 2010). The main development region (MDR) can be found from approximately 10° to 20°N latitude and extends westward from the West African coastline to Central America. Tropical disturbances typically form to the west of 30°W and are found to the south of Cape Verde. However, during the 2006 NAMMA campaign, TS Debby and Tropical Depression 8 formed to the east of 30°W (Zipser et al. 2009). The role of Saharan dust through aerosol–cloud microphysics interactions and the impacts on rain properties in relationship to the genesis of tropical cyclones emerged as a relevant topic from the NAMMA field campaign. A related field campaign to NAMMA, funded by the United Kingdom, took place during the summer of 2015 and was called the Ice in Clouds Experiment–Dust (ICE-D). It aimed to examine aerosol–cloud microphysics and

precipitation processes in layered and cumulus clouds. The British Aerospace 146 (BAe 146) aircraft and science team were deployed in Praia, Santiago, Cape Verde, during the period of 4–25 August 2015 with limited upper-air, dust, and ozone measurements in Sal, Cape Verde, where a hydrogen generator is located at the National Institute for Meteorology and Geophysics (INMG).

Although tropical disturbances can be organized as they approach Cape Verde, the first record of hurricane-force winds in modern times was not until August 2015, when Fred passed through the center of the country. The only other hurricane to have impacted Cape Verde occurred on 13 September 1892. The National Hurricane Center's (NHC) "best track" hurricane database HURDAT2 (Landsea et al. 2013) suggests that this tropical cyclone passed north of the Sotavento islands but remained south of the Barlavento islands. As a tropical storm, the closest approach would have been near the island of Boa Vista, and it is estimated to have reached hurricane status south of São Nicolau over water. However, rainfall records show very small amounts of rain in Mindelo (São Vicente) and Praia Vila (Santiago), suggestive of a weak tropical cyclone with minimal impact on Cape Verde.

Since 1892 the HURDAT2 database indicates that Cape Verde has been directly impacted by 15 tropical disturbances, including seven tropical depressions (1934, 1958, 1964, 1967, 1984, 1987, and 1989), five tropical storms (1893, 1901, 1924, 1927, and 1961), and two hurricanes (1892 and 2015). In addition, there have been numerous events that have not passed through, but moved very close to, the Cape Verde islands, such as Tropical Storm 3 in 1923, which caused reported damage. More recently, TS Debbie (1961), TS Beryl (1982), TS Fran (1984), TS Julia (2010), TS Humberto (2013), and Hurricane Fred (2015) have come close to or impacted Cape Verde.

The close proximity of Cape Verde to West Africa's coast and the potential genesis and rapid development of a tropical cyclone presents a real challenge to forecasters who must protect the population across a diverse landscape. Flash flooding in mountainous regions from heavy hurricane rainfall and coastal flooding for the 10 islands are examples of these challenges. More importantly, while there is some experience with tropical storms (1982, 1984), the population has no experience from a recent hurricane. Consequently, uncertain decision-making by the public is possible because of limited experiences with the various dangers associated with a hurricane. In addition, damage from a hurricane can have negative consequences for economic development in Cape Verde.

On 31 August 2015, satellite images and surface data show that Hurricane Fred passed through the Cape Verde islands, possibly making landfall in eastern parts of São Nicolau at approximately 1800 UTC, as shown by the NHC best track data in Figs. 2a and 2b. Limited observations and no weather radars in Cape Verde do not allow for absolute verification of landfall, but model forecasts and station observations suggest that Hurricane Fred could have made landfall in eastern São Nicolau during the late afternoon of 31 August. The NHC estimates that Tropical Cyclone (TC) Fred was a hurricane from 0000 UTC 31 August through 0000 UTC 1 September, with maximum winds of 75 knots (1 kt = 0.51 m s^{-1}) and a pressure of 986 hPa at 1200 UTC (Beven 2016). Our objectives are to 1) describe the weather guidance and subsequent actions related to public protection prior to Hurricane Fred; 2) present surface and upper-air observations from Cape Verde, which were not available during the event, along with the Weather Research and Forecasting (WRF) Model forecast of Hurricane Fred on 31 August; 3) discuss impacts from Hurricane Fred on Cape Verde; and 4) discuss the lessons learned and recommendations for improvements in the observing and communication systems and annual hurricane planning activities.

THE FORECAST AND PREPARATION FOR TROPICAL CYCLONE FRED. On 27 August 2015, the National Centers for Environmental Prediction (NCEP) Global Forecast System (GFS) model forecasted a disturbance to exit West Africa and move toward the Cape Verde islands. The coarser-grid NCEP reanalysis depicts the 850-hPa center over southern Burkina Faso (11°N, 3°W) at 0000 UTC 28 August and enters eastern Guinea at 1200 UTC, with *Meteosat-10* infrared (IR) brightness temperatures (Janowiak et al. 2001) less than 220 K to the west of the 850-hPa center (Figs. 3a,b). At 1200 UTC 29 August, NCEP reanalysis shows that the 850-hPa center is located off the coast of Guinea-Bissau, with IR brightness temperatures less than 220 K, especially in eastern parts of the vortex (Fig. 3c). At 1200 UTC 30 August, NCEP reanalysis shows the 850-hPa center near 12°N, 24°W with convection on its eastern flank (Fig. 3d). The NCEP reanalysis position is to the southwest of the position determined by NHC at the time it named Tropical Storm Fred near 13.1°N, 19.5°W (Fig. 2b). Sea surface temperature (SST) anomalies are up to 2°C above normal between coastal West Africa and Cape Verde during the week of 31 August (www.ospo.noaa.gov/Products/ocean/sst/anomaly/2015.html).

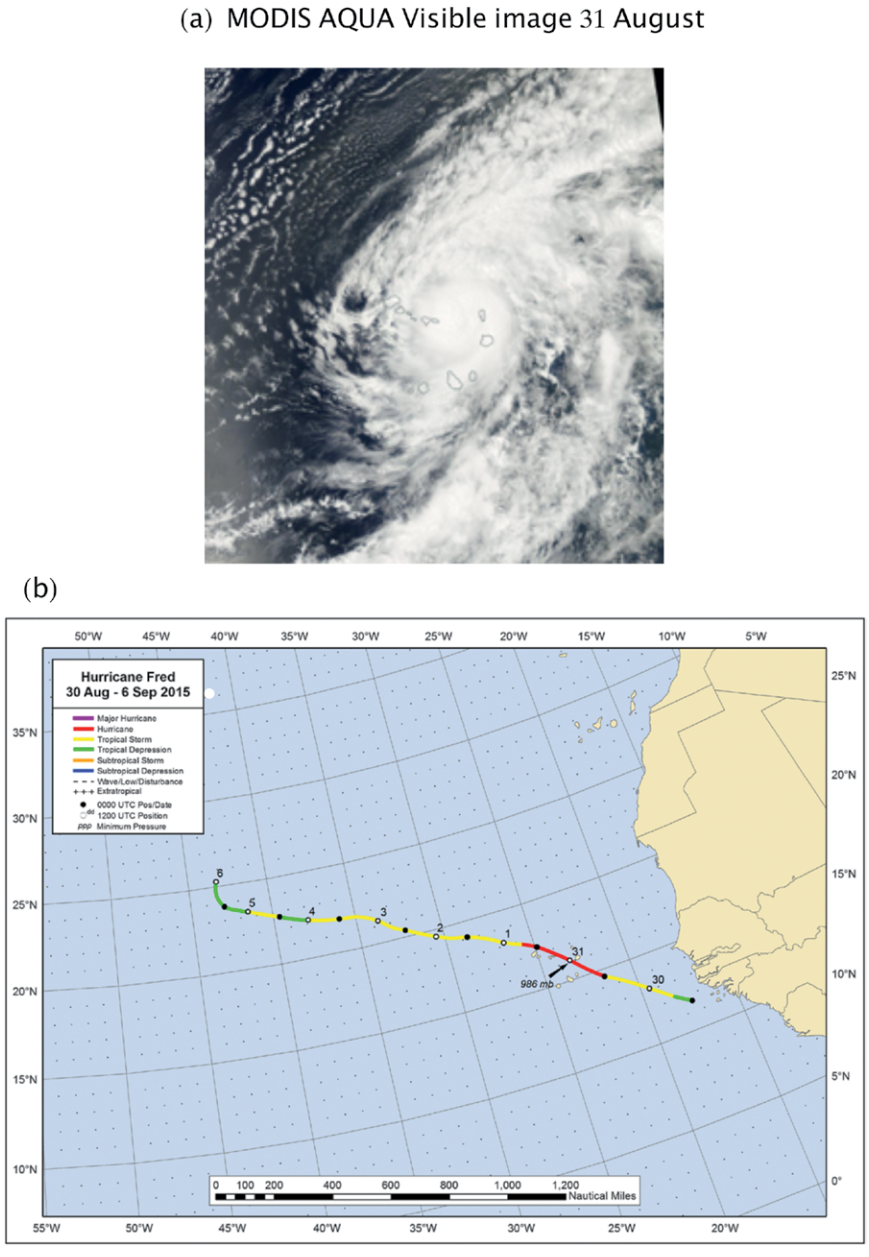

Fig. 2. (a) *Aqua* Moderate Resolution Imaging Spectroradiometer (MODIS) 31 Aug 2015 visible image of Hurricane Fred. (b) Best track from the NHC for Hurricane Fred.

As a result of the GFS and WRF forecasts (discussed below), the leadership team at INMG and forecasters began to have meetings on 28 August to discuss the disturbance and plans for alerting the government and civil protection authorities [formally Serviço Nacional de Protecção Civil (SNPC)]. Additional upper-air measurements at 0000 UTC were planned for 29, 30, and 31 August, with the data directly sent to the NHC. Daily meetings continued on 29 and 30 August, with communications sent to the SNPC. To address potential dangers to vulnerable populations and to address potential disruptions in services, the leadership at INMG met with local authorities, SNPC, media (radios and national television), Red Cross representatives, and military personnel on the island of Sal. Alerts and advisories were issued to the other islands (Maio and Boa Vista), which allowed authorities and the population a limited amount of time to prepare for the possibility of a tropical cyclone.

The NHC advised the public on the possibility of a tropical depression to develop over the next 5 days prior to the disturbance emerging from West Africa. The probability of a tropical storm forming increased on 29 August, with statements advising residents of the Cape Verde islands to stay alert to the possibility of tropical cyclone formation. Tropical Depression 6 was identified at 0530 UTC 30 August and was upgraded to Tropical Storm Fred at 0900 UTC; subsequently, a tropical storm warning and a hurricane watch were posted for the Cape Verde islands (Beven 2016). Tropical Storm Fred was upgraded to Hurricane Fred at 0000 UTC 31 August, and a hurricane warning was in effect for all of the Cape Verde islands.

As Tropical Storm Fred approached the Cape Verde islands, model guidance became better with respect to the track and intensity. However, because of the short distances among the islands of Cape Verde (less than 2.5° latitude–longitude), small deviations in the projected path could have significant consequences, especially for those islands near the track. The models were generally projecting the storm to the east of Santiago, but to the west of Boa

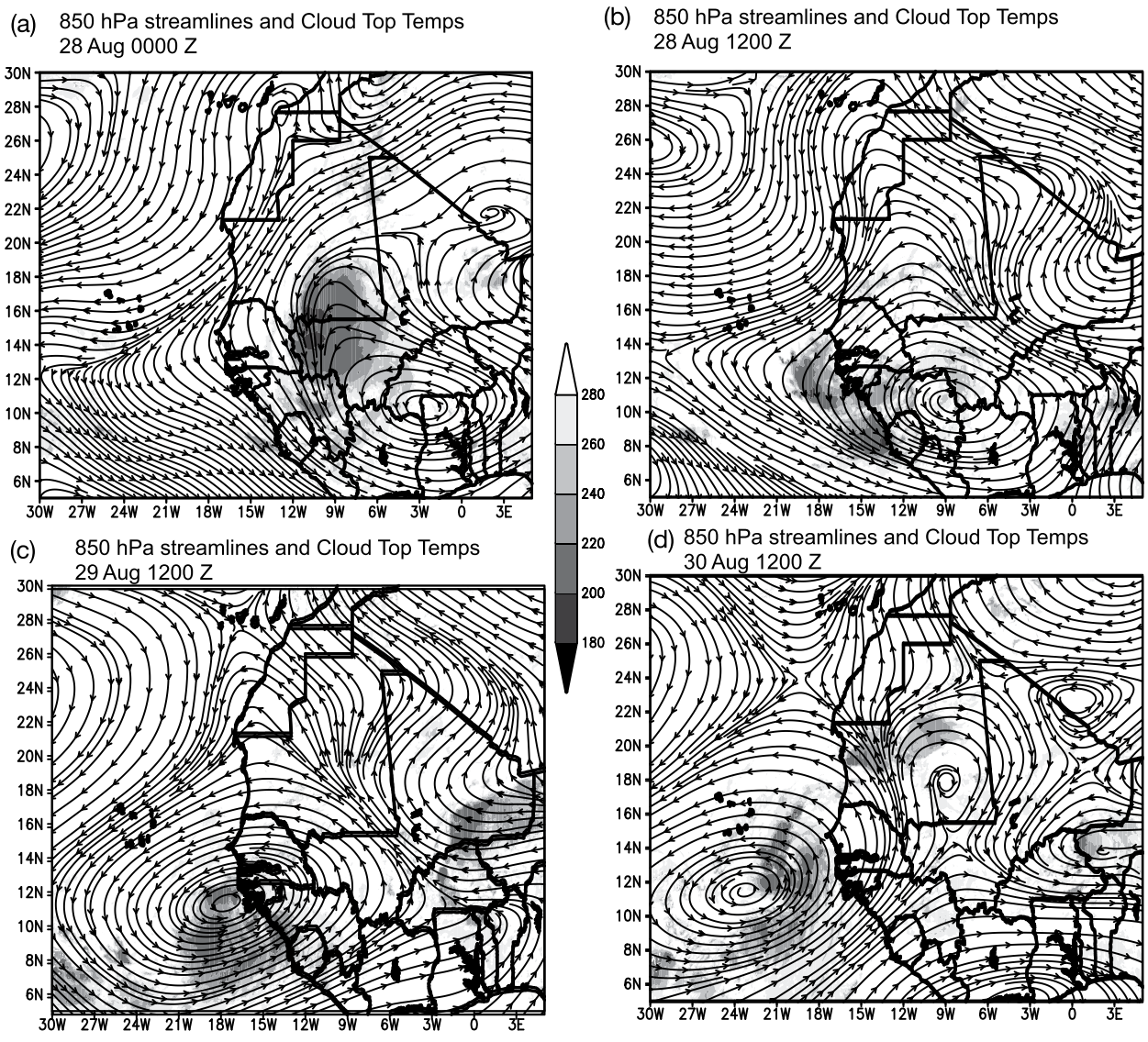

Fig. 3. NCEP reanalysis 850-hPa streamlines and IR brightness temperatures (K).

Vista and Sal, with the cone of uncertainty increasing toward the northern islands. Of great concern were the northern islands, where there was the potential for hurricane-force winds and life-threatening flash floods in the mountainous regions of western São Nicolau (elevation >1,000 m) and central Santo Antão (elevation 1,500–2,000 m). NHC warned of life-threatening flash floods and mudslides, rainfall amounts of 3–5 in. (76.2–127 mm) with possibly as much as 8 in. (203 mm), and a storm surge causing coastal flooding, and large/dangerous waves. Even with guidance from the models, the cone of uncertainty still left the northern islands within the impact zone of Tropical Storm or Hurricane Fred.

OBSERVATIONS AND EVALUATION OF WRF GUIDANCE. *Observations.* Figures 4a–d show an area of IR brightness temperatures (<220 K) associated with Hurricane Fred during 31 August (Janowiak et al. 2001). At 0600 UTC the storm center is south of Boa Vista near the lowest temperature (<200 K), with convection extending to the west over Santiago (Fig. 4a). At 1200 UTC, Santiago, Maio, Boa Vista, and Sal are under the influence of convection, with the center of Hurricane Fred located due west of Boa Vista (Fig. 4b). At 1800 UTC, Hurricane Fred is located northeast of São Nicolau, with the *Meteosat-10* IR brightness temperatures of less than 200 K found near the center; São Nicolau, São Vicente, and Santo Antão are under the influence of convection (Fig. 4c). By 0000 UTC, now downgraded, Tropical Storm Fred is located north of São Vicente, with convection still affecting Santo Antão, São Nicolau, and São Vicente (Fig. 4d).

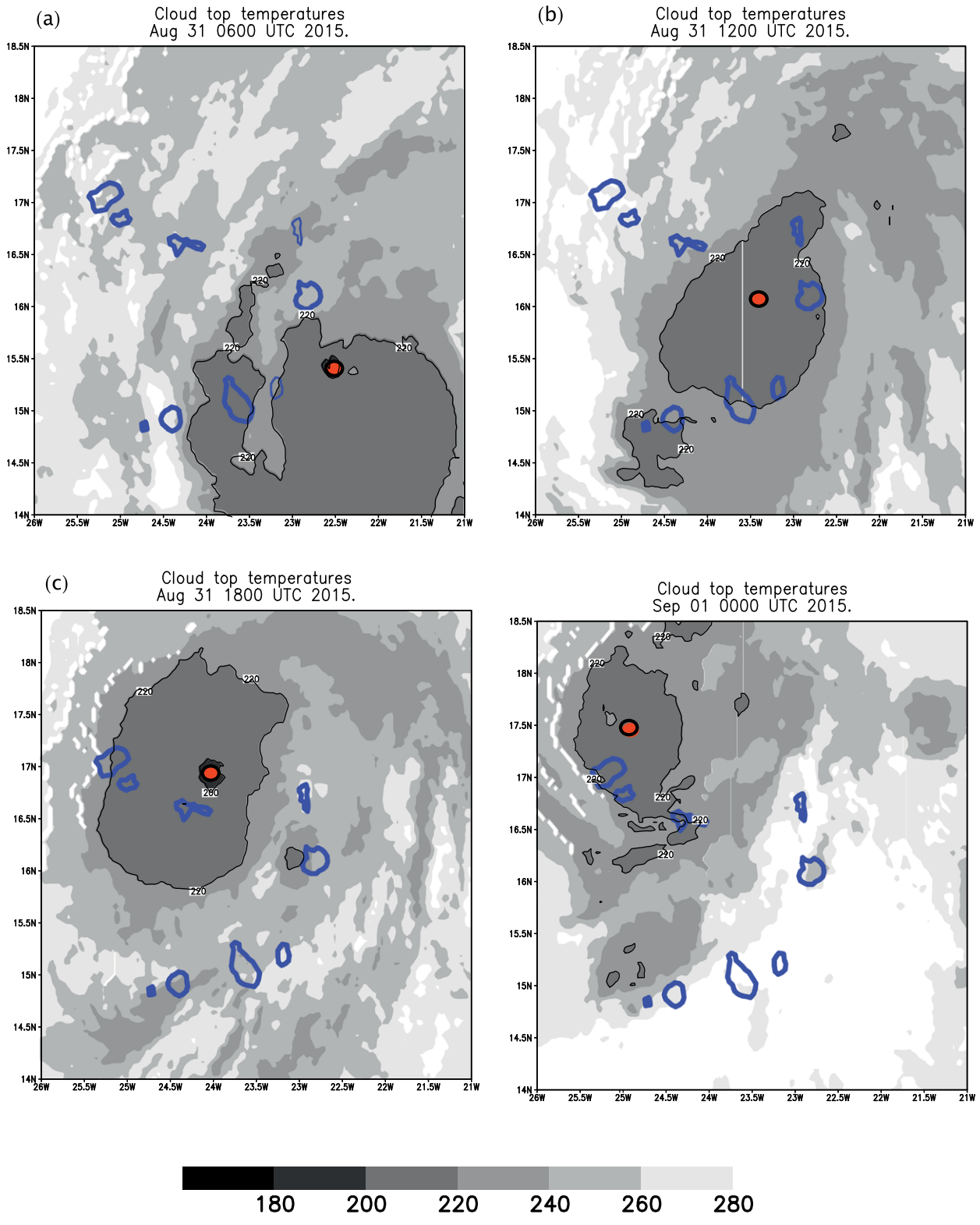

Fig. 4. IR brightness temperatures (K) and location (red circle) of TC Fred at (a) 0600, (b) 1200, and (c) 1800 UTC 31 Aug and (d) 0000 UTC 1 Sep.

Daily satellite-based rainfall estimates from the Global Precipitation Measurement (GPM) satellite, Integrated Multisatellite Retrievals for GPM (IMERG) product, and Tropical Rainfall Measuring Mission (TRMM) Multisatellite Precipitation Analysis (TMPA), which uses available satellite

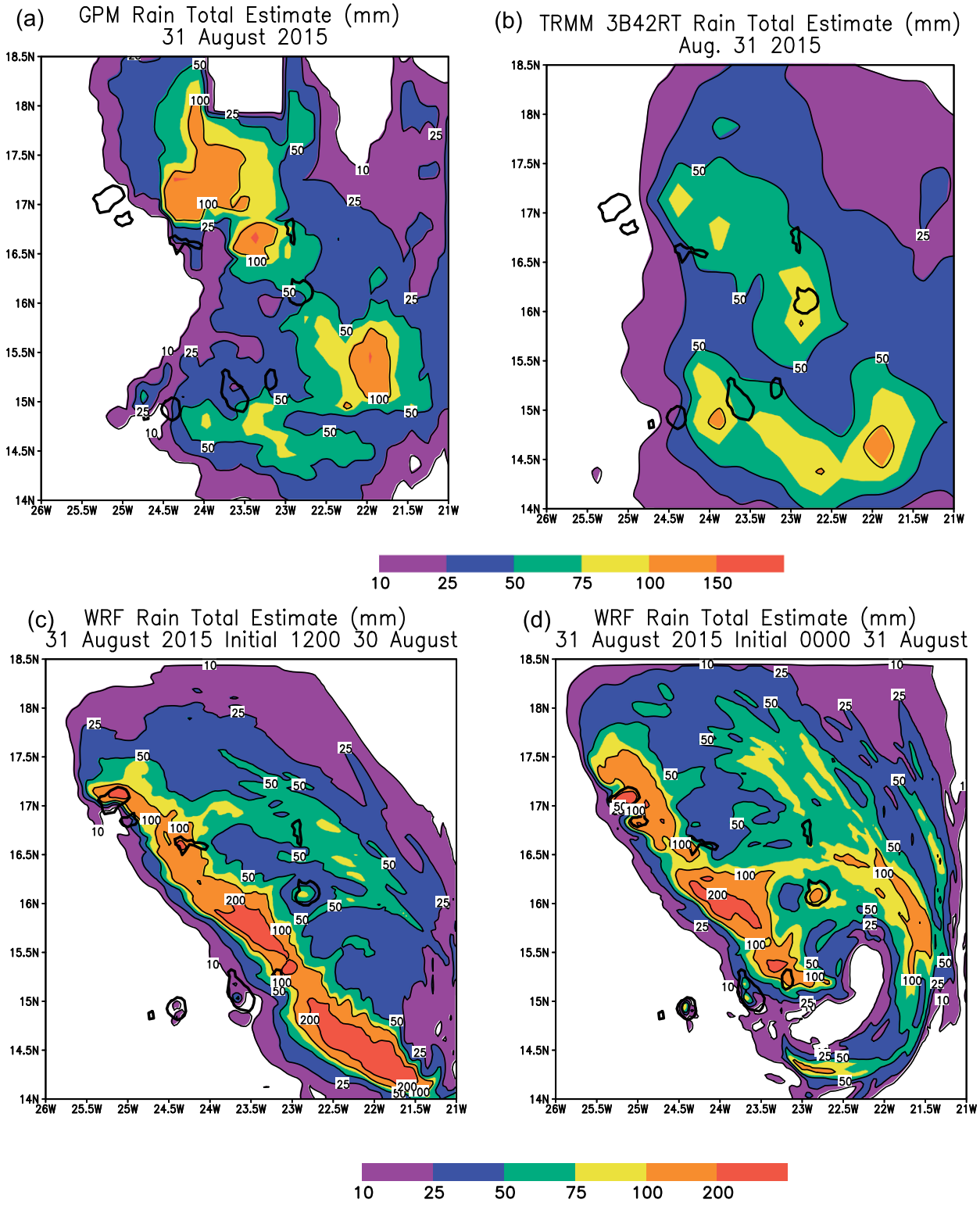

Fig. 5. Rainfall totals (mm) for 31 Aug from (a) IMERG and (b) TMPA, (c) WRF forecast 1200 UTC 30 Aug initializations, and (d) WRF forecast 0000 UTC 31 Aug initializations.

infrared and microwave data and surface observations (Huffman et al. 2007; TRMM was no longer operational in August 2015), show rain amounts exceeding 100 mm on 31 August (Figs. 5a,b). The GPM estimates show most of the heavy rain falling over the ocean, with the highest rain amounts of 50–100 mm occurring over Boa Vista and Sal. TMPA estimates show similar rainfall amounts, but with

Table 1. Rainfall totals (mm) and maximum winds (kt) across Cape Verde on 31 Aug and 1 Sep.

Island	Avg rain	Min rain	Max rain	Max wind	No. of stations (rain)
São Filipe	127	65	200	—	20
Santiago	96	20.6	330.3	26	29
Maio	53.1	40	69	—	7
Boa Vista	73.6	42.3	96	52.9	5
Sal	53.6	24.3	87	36	4
São Nicolau	45.5	26.2	90	69	2
São Vicente	29.9	19.5	38	31.7	6
Santo Antão	158.2	97	330	16.8	20

the southern islands of Santiago and Maio receiving 50–100 mm.

The rain gauge network and automated weather stations were not available in real time, but they were analyzed after the passage of Hurricane Fred and provided surface quantitative estimates of rainfall impacts across the Cape Verde islands on 31 August. Rain gauges show that São Filipe, Santo Antão, and Santiago all received approximately 100–150 mm of rain on 31 August (Table 1). These three islands have mountainous areas, with some stations measuring rain amounts of 200–330 mm. São Nicolau experienced problems with the automated stations, resulting in no station reports in mountainous areas, but it is very likely that these areas received more than the reported 90 mm of rain at Juncalinho. In addition, Table 1 shows that tropical-storm-force winds were measured in Boa Vista (53 kt) and Sal (36 kt), while hurricane-force winds were reported at the airport in São Nicolau (69 kt) based on 1-min averages.

Figure 6 shows 10-m wind speeds and station pressure from automated stations on the islands of Santiago, Boa Vista, Sal, São Nicolau, São Vicente, and Santo Antão. The maximum winds are correlated to Hurricane Fred's location, with the lowest station pressures occurring at Santiago, Boa Vista, and Sal during the morning hours of 31 August and at São Nicolau at approximately 1800 UTC. Maximum winds at São Vicente and Santo Antão occurred during the late evening hours of 31 August or early morning hours of 1 September. The strongest winds recorded in the Cape Verde islands occurred at Preguiça Airport on São Nicolau, with 1-min data showing hurricane-force winds (69 kt) and a station pressure of 997.5 hPa occurring at 1820 UTC (see online supplemental Fig. ES1: https://doi.org/10.1175/BAMS-D-16-0222.2). Boa Vista and Sal both received tropical-storm-force winds for significant periods of time, with peak wind speeds at Boa Vista occurring at approximately 1000 UTC. The steepest station pressure reductions of 12–17 hPa occurred at Boa Vista and São Nicolau as Hurricane Fred approached, although significant pressure drops are also found at São Vicente and Santo Antão.

Figures 7a–c show the vertical profiles of relative humidity, wind speed, and wind direction at Sal during the period from 28 August through 1 September. From 28 to 30 August, the SAL (Carlson and Prospero 1972) was in place in the lower to middle troposphere, with relative humidity values less than 10% near 900 hPa (Fig. 7a). However, relative humidity values steadily increase beginning at 0000 UTC 31 August, with a moist profile throughout the troposphere at 1200 UTC 31 August and 0000 UTC 1 September. While there is evidence of the AEJ near 600 hPa on 28 August with the SAL, strong winds associated with Hurricane Fred show maximum values of 55 kt near 850 hPa near 0900 UTC 31 August and remain above 40 kt at 0000 UTC 1 September (Fig. 7b). Throughout the period leading up to Hurricane Fred, winds in the lower to middle troposphere have a north to northeasterly direction (Fig. 7c). The passage of Hurricane Fred leads to a shift to southerly winds throughout the troposphere at Sal.

WRF forecasts of Hurricane Fred. We have used various versions of WRF (Skamarock et al. 2008) since the AMMA field campaign (Chiao and Jenkins 2010), providing real-time forecast guidance in West Africa and Cape Verde. For this work, we use version 3.4 of the WRF Model, with the parent domain covering much of West Africa with a grid spacing of 12 km and a second nested domain with 3-km grid spacing covering Cape Verde. The finer grid spacing allows for an accurate representation of each island and orographic features. The parent domain is 283 east–west grid points, 181 north–south grid points, and 31 vertical levels; the nested domain is 196 east–west grid points, 160 north–south grid points, and 31 vertical levels. The NCEP GFS is used to initialize and provide boundary conditions for the 72-h WRF forecast. Two-way feedback is used between the outer and inner domains, and no cumulus

▸ Fig. 6. Station pressure (hPa) and wind speeds (kt) from Cape Verde for (a) Praia, (b) Boa Vista, (c) Sal, (d) São Nicolau, (e) São Vicente, and (f) Santo Antão.

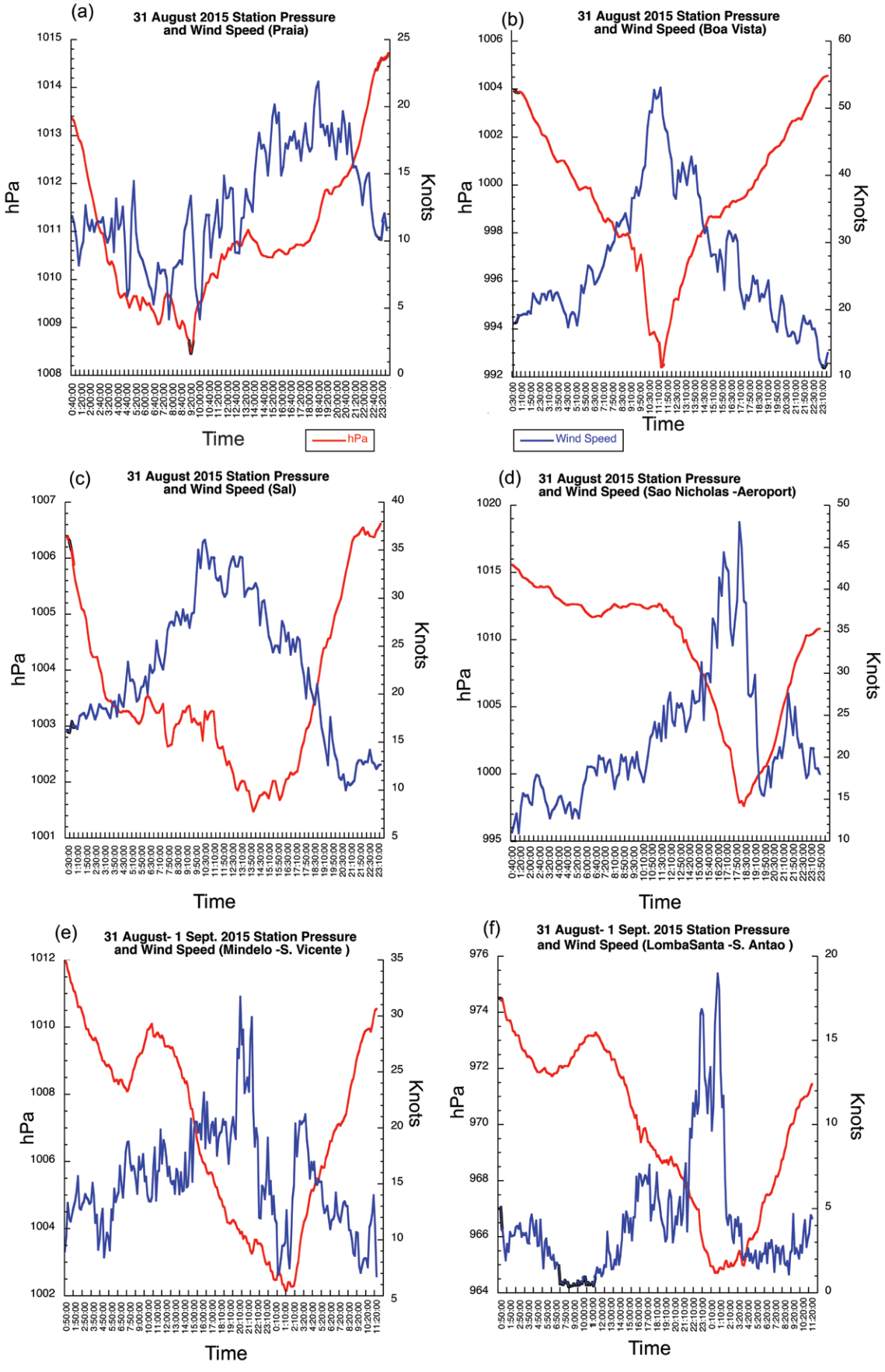

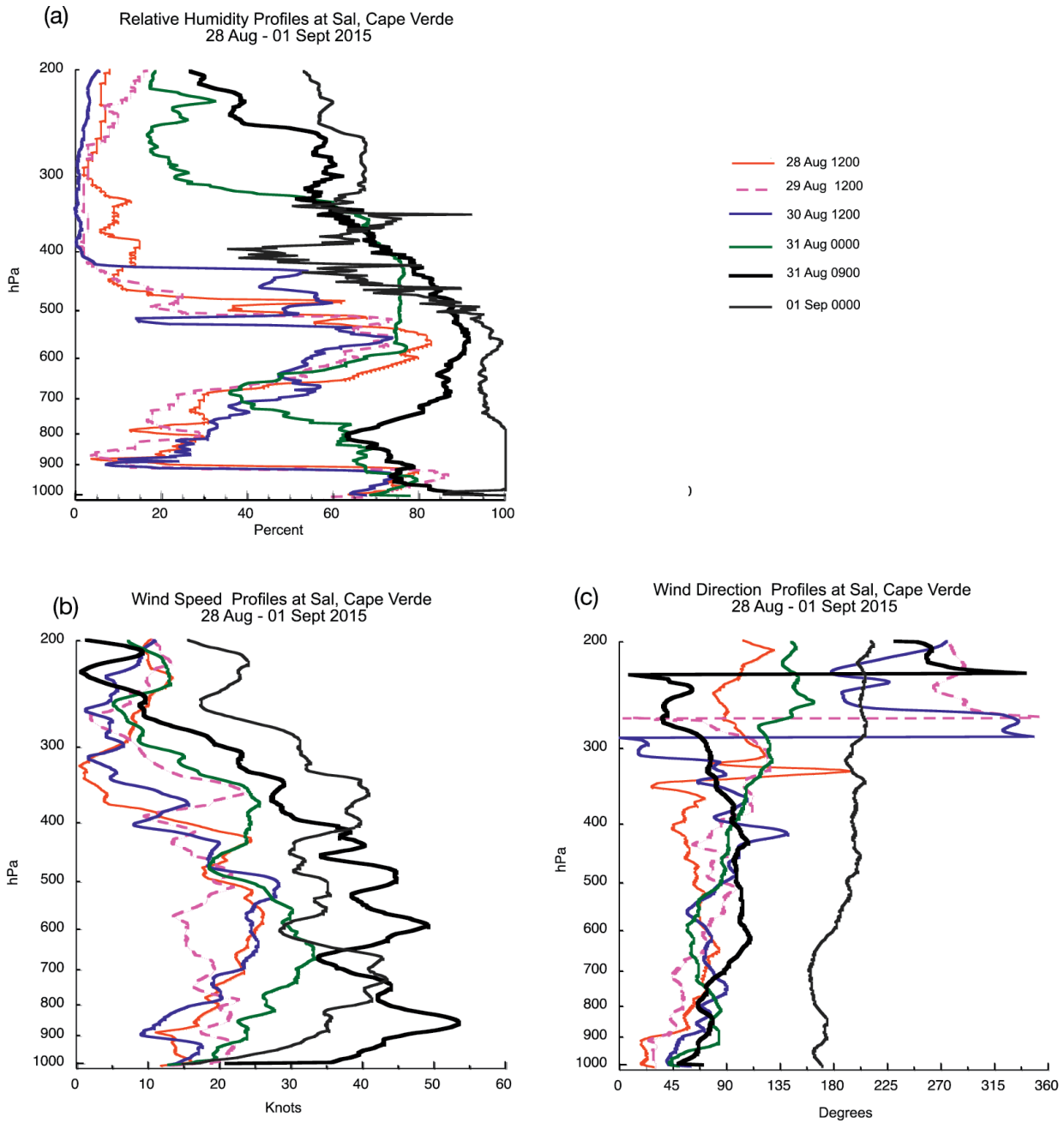

Fig. 7. Vertical profiles of (a) relative humidity, (b) wind speeds, and (c) wind direction from Sal, Cape Verde.

parameterization is used for the 3-km grid. Prior to Hurricane Fred's formation, we used WRF forecasts, other models [GFS, Canadian (http://moe.met.fsu.edu/tcgengifs/), European Centre for Medium-Range Weather Forecasts (ECMWF)], and the NHC Tropical Weather Outlook and discussion products for guidance in our discussions of TC Fred.

Figures 5c and 5d show the heaviest precipitation amounts (>200 mm) associated with Hurricane Fred in the western Cape Verde islands (Figs. 5c,d) based on forecasts initialized at 1200 UTC 30 August and 0000 UTC 31 August. However, the WRF Model severely underestimated rain totals for the southern islands of Santiago and São Filipe based on observed values (Table 1).

Figures 8, 9a, and 9b show the NHC location (red circle) and WRF forecasts of sea level pressure (SLP) and winds speeds (kt) at 1200 and 1800 UTC 31 August. Less than 24 h before TC Fred impacted Cape Verde, the 1200 UTC 30 August forecast was the primary WRF forecast, along with NHC guidance and other model output for discussion by our team in

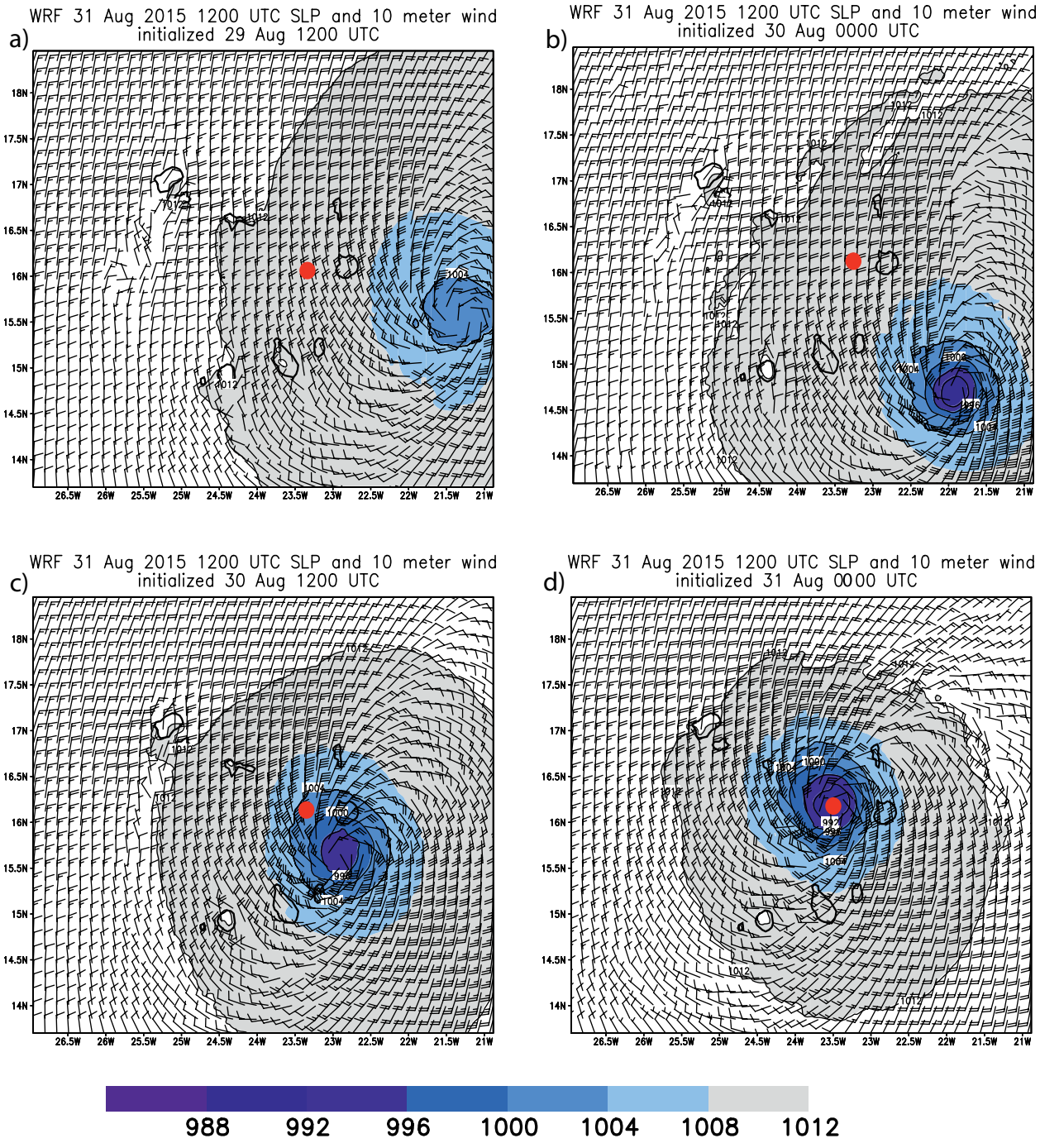

Fig. 8. The 1200 UTC 31 Aug WRF forecast of TC Fred from initialized forecasts at (a) 1200 UTC 29 Aug, (b) 0000 UTC 30 Aug, (c) 1200 UTC 30 Aug, and (d) 0000 UTC 31 Aug. The red circle represents the approximate NHC location of Fred.

examining the potential track, wind intensity, and rain estimates, in part because of its finer resolution. Figure 8 shows the forecasted location of TC Fred at 1200 UTC 31 August for the four initialized forecasts between 1200 UTC 29 August and 0000 UTC 31 August. The early WRF forecasts at 1200 UTC 29 August and 0000 UTC 30 August, show the largest biases in location relative to the NHC estimated location at 1200 UTC 31 August (Figs. 8a,b). These forecasts show an eastward bias of several hundred kilometers, which narrowed to less than 150 km in the 1200 UTC 30 August and 0000 UTC 31 August forecasts (Figs. 8c,d). At 1200 UTC, winds at Boa Vista were blowing from the east-southeast (100°), while the WRF 1200 UTC 30 August

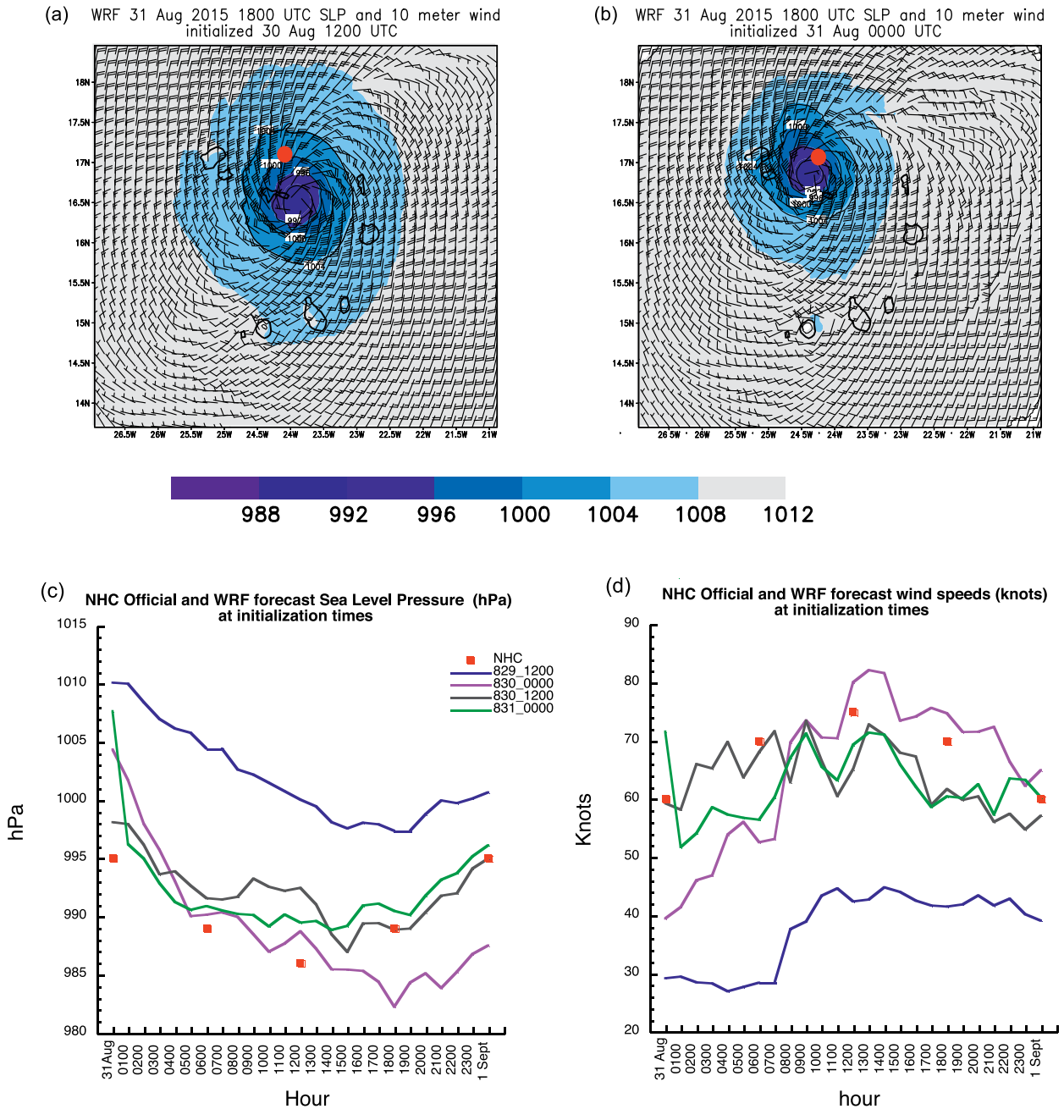

Fig. 9. The 1800 UTC 31 Aug WRF location, SLP (hPa), and 10-m wind field (kt) of TC Fred from initialized forecasts at (a) 1200 UTC 30 Aug and (b) 0000 UTC 31 Aug. The red circle represents the approximate NHC location of Fred. (c) Evolution of SLP and (d) 10-m wind speeds from WRF forecast initialized between 1200 UTC 29 Aug and 0000 UTC 31 Aug.

forecast predicted winds from the northeast and the 0000 UTC 31 August forecast predicted winds from the south. The 0000 UTC 31 August forecast suggested that Hurricane Fred may have been located farther east than the official NHC estimated location.

The 1800 UTC forecasts of Hurricane Fred show the eastern parts of São Nicolau being significantly impacted in the 1200 UTC 30 August and 0000 UTC 31 August initialized forecasts (Figs. 9a,b). The 1-min surface observations at the São Nicolau airport (16.35°N, 25.5°W; elevation 204 m) show hurricane-force winds and wind gusts between 1759 and 1823 UTC (see Fig. ES1). Satellite IR brightness temperatures and surface observations suggest that Hurricane Fred underwent slight strengthening during the afternoon of 31 August. The wind observations from São Nicolau show the lowest pressures of approximately 997 hPa between 1751 and 1810 UTC, with a 1-min

Table 2. Estimated damages in Cape Verde from Hurricane Fred. (Source: Camaras Municipais e Instituto de Estradas: http://ine.cv/en/; currency exchange of the day: 1 USD = 101,077 CVE.)

Island	Damage	Additional items (estimated costs CVE)	Additional items (estimated costs USD)
Santiago	Pavement, supporting walls, road protection	87,000,000	860,728.94
Fogo	Pavement, supporting walls, road protection	5,200,057	51,446.49
Boa Vista	House roofs, building covers and walls, pavement, road protection, supporting walls, dikes	44,028,000	435,588.71
Sal	Santa Maria Pier, high school cover	30,000,000	494,672.38
São Nicolau	Landslides, house roofs, agriculture, electricity and telephone poles, falling trees, pavement, road protection, supporting walls	50,527,924	499,895.37
São Vicente	House roofs, electricity and telephone poles, falling trees	4,000,000	39,573.79
Santo Antão	Pavement, road protection, supporting walls	12,146,644	120,172.19
	Total	2,529,026,525	2,502,078.86

wind speed range of 31–61 kt. The strongest winds of 69 kt from the north were recorded at 1820 UTC (see Fig. ES1). The best forecast evidence of a possible landfall in eastern São Nicolau comes from the WRF forecast initialized at 1200 UTC 30 August, which indicates Hurricane Fred is near eastern São Nicolau at 1800 UTC. The forecast initialized at 0000 UTC 31 August shows Hurricane Fred near eastern São Nicolau between 1500 and 1600 UTC, a few hours earlier than the station observations.

The WRF forecasts of SLP and 10-m wind speeds from 1200 UTC 29 August through 0000 UTC 31 August are compared to NHC 6-h estimates in Figs. 9c and 9d. The NHC official storm estimates show SLP values in the 985–995-hPa range and wind speeds of 60–75 kt during 31 August. Only the 1200 UTC 29 August WRF forecast predicts weak tropical storm conditions.

All WRF forecasts after 0000 UTC 30 August predict hurricane-force winds for Hurricane Fred. The 0000 UTC 30 August forecast predicts the strongest hurricane, with a minimum SLP of 983 hPa and winds of 83 kt during the late afternoon of 31 August (Figs. 9c,d). However, this forecast had a large southwest bias relative to the NHC location at 1200 UTC 31 August (Fig. 8b). The next two forecasts at 1200 UTC 30 August and 0000 UTC 31 August show similar values of minimum SLP (995–990 hPa) during the afternoon of 31 August. A double peak in maximum winds (72 kt) is found during late morning and mid- to late afternoon in both forecasts (Figs. 9c,d). Hurricane-force winds are forecasted in the 1200 UTC 30 August forecasts by 0200 UTC and last through 1700 UTC. The 0000 UTC 31 August forecast shows hurricane-force winds from 0800 UTC through 1700 UTC (Fig. 9d).

DAMAGE REPORTS ASSOCIATED WITH FROM HURRICANE FRED. A summary of damage from Hurricane Fred in Cape Verde shows that on 31 August and 1 September, 7 of the 10 islands were significantly impacted (Table 2). Damage reports from Cape Verde show that the islands of São Filipe (Fogo), São Vicente, and Santo Antão received the least amount of damage. Islands where the winds were strongest (Boa Vista, São Nicolau, and Sal) had damage estimates of $400,000 to $500,000, with the most extensive damage occurring in Boa Vista and São Nicolau. While the lowest winds speeds are observed in Santiago, the cost of damage from Hurricane Fred is the largest because of the heavy rainfall, as noted in Table 1. There were officially no fatalities in Cape Verde associated with Hurricane Fred.

Additional damage and fatalities occurred to the south of Cape Verde prior to 31 August before Tropical Storm Fred formed. This includes the capsizing of a fishing vessel off the coast of Guinea-Bissau, leading to seven fatalities (three from Senegal, two from Guinea-Bissau, one from Sierra Leone, and one from Cape Verde). In addition, strong seas battered the coast of Senegal, leading to damage between the cities of Mbour and Dakar. Damage was reported in coastal locations, including the district of Hann, which is located within Dakar. Numerous homes and fishing vessels in the fishing village of Barny, Senegal (located 35 km from Dakar), were extensively damaged or destroyed. The damage and fatalities prior to Hurricane Fred's formation are similar to the disturbance that formed prior to Tropical Storm Cindy in 1999 (Sall and Sauvageot 2005).

LESSONS LEARNED FROM HURRICANE FRED. On 31 August 2015, the island nation of Cape

Verde experienced its first hurricane in modern times. Property damage occurred, but there were no fatalities in part due to the fortuitous track of Hurricane Fred through Cape Verde and warnings by the civil protection. The track of Hurricane Fred missed the large population (300,000 residents) on the island of Santiago (and its capital, Praia), and the westward turn of Hurricane Fred after moving north of São Nicolau may have averted catastrophic damage in São Nicolau, São Vicente, and Santo Antão, where strong winds, heavy precipitation with flash flooding, dangerous waves, and surge would have increased damage and may have caused fatalities. The close proximity of Cape Verde to coastal West Africa, where tropical cyclone formation is possible but does not occur frequently, may limit preparedness and awareness of dangerous hazards. There are a number of important lessons and recommendations that emerged from Hurricane Fred that we discuss next.

Improving the communication of risk to stakeholders with different languages, cultures, and livelihoods. The communication of threats from tropical disturbances is required along coastal West Africa from Guinea to Cape Verde, where languages vary among French (Guinea, Senegal), English (Gambia), Portuguese (Guinea-Bissau, Cape Verde), and local languages. These languages are spoken in established West African coastal and Cape Verde fishing communities where there is small-scale fishing and larger-scale fishing operations occurring each day in addition to ferry transportation and commercial shipping. Hence, clear communication of threats from a tropical disturbance must be relayed in different languages for local stakeholders. Civil protection authorities must be made aware of tropical cyclone threats to coastal villages and cities for effective emergency management (e.g., evacuation, search and rescue). All existing communication forms should be utilized (television, radio, Internet, social media, text messages) to alert the population, and government officials should be equipped with the proper communication tools when there is a loss of power and telephone services.

Annual hurricane planning. Hurricane Fred is a reminder that annual hurricane planning is required for Cape Verde and coastal zones of West Africa. Long periods between tropical cyclones making landfall in Cape Verde can increase the vulnerability of its population. In the case of Hurricane Fred, the favorable track where a direct strike on any island was not observed and actions by the civil authority may have reduced the loss of life in Cape Verde. Still, challenges for preparedness include language, culture, local factors (e.g., poor drainage or mudslide potential), and a clear understanding of what each individual should do when faced with a particular hazard (flooding, storm surge, wind damage). These challenges can be addressed through annual hurricane awareness programs by the civil protection authorities to the general population, especially those in vulnerable regions (mountainous regions, coastlines, or isolated regions on islands) or for livelihoods (fisheries and commercial shipping) where there is risk. The NHC hurricane awareness program can serve as a model that can be adapted to Cape Verde and coastal West Africa with materials produced in Portuguese, French, and local languages. The national meteorological services in concert with the National Hurricane Center and civil protection authorities can deliver the products. As an initial step in Cape Verde, a forecaster from INMG spent a week at NHC, and a visit by NHC specialists is planned in the near future to assist with hurricane awareness and preparedness.

Improving the observing system and forecasts. Upper-air measurements. Sal, Cape Verde, is the westernmost upper-air station in the eastern tropical Atlantic and along with Dakar, Senegal, provides important information on easterly waves and the SAL. Sal provides observations at 1200 UTC; however, the semiarid conditions at the airport (59.6 mm yr^{-1} for 1981–2010) are not reflective of more humid conditions in the southern parts of Cape Verde, such as the Praia Nelson Mandela International Airport (164.5 mm), where most of the rain falls from late August through October. The SAL dominates the profiles of Sal during the Northern Hemisphere summer, but it is not clear how frequently dry air enters the southern islands; thus, radiosonde measurements would be useful in the Sotavento islands (Santiago, Fogo, and Brava). Upstream over Africa, an increase in frequency of stations with twice-per-day measurements is required for better initialization of global weather models.

Precipitation measurements. There are currently no weather radars within Cape Verde. Having radar capability would assist in determining the center of a tropical disturbance and would provide details on precipitation structure, both of which are critical information to NHC. The radar measurements can provide real-time information for the civil authorities in planning emergency efforts. The radar measurements can provide estimated rain accumulation in real time for civil authorities, which can facilitate in decision-making for planning emergency efforts such as search and rescue

efforts. At a minimum, real-time transmission from automated stations using mobile phones should be used to estimate rainfall, especially in flood-prone areas.

Ocean measurements. Coastal regions of West Africa and Cape Verde are void of ocean buoys, which are required in measuring the state of the ocean while providing meteorological estimates of winds speeds and direction and SLP for tropical disturbances. The buoy data (SSTs, wave heights) are critically needed for ocean search and rescue missions by civil protection authorities. The buoys are necessary for determining the biases in ocean and meteorological model forecasts in the genesis stages of potential tropical cyclones. Reductions in the biases will increase our understanding of processes and improve confidence in forecasts.

Forecasts of TC genesis and intensity over the extreme eastern Atlantic. AEWs are the source of most tropical cyclones that will form over the eastern Atlantic. While the locations of AEWs are forecasted very well, the weather associated with the waves and the potential tropical cyclogenesis needs improvement. Accurate TC genesis forecasts with good initial conditions are required because of the close proximity between the Cape Verde islands and coastal West Africa, which can provide decision-makers and the public additional lead time. Finescale forecasts are also required because of the relatively small spatial distances among the Cape Verde islands and steep orography (resolved by WRF 3-km grid spacing) for determining impacts. In addition, the national meteorological services need forecasts of precipitation rates and amounts, wind speeds, gusts, coastal surge, and wave heights associated with AEWs and potential tropical disturbances.

Because of the diversity in land surface heterogeneity across the Cape Verde islands, topography, and population sizes, determining the degree of confidence in the forecast of potential hazardous weather associated with tropical cyclones is also important. This includes the timing, duration, intensity, and location of a tropical cyclone for decision-makers to take action for protecting life and property. For example, Hurricane Fred moved faster than anticipated and turned westward after passing São Nicolau, with the cone of uncertainty providing limited guidance because of the small distances among the northern islands. Consequently, there was significant discussion related to potentially dangerous conditions at São Nicolau, São Vicente, and Santo Antão and the impacts prior to 31 August. However, a major challenge is related to forecasting the locations of extreme rain amounts. In the case of Hurricane Fred, the models did not predict the flooding associated with the outer rainbands over the southerly islands (Santiago, São Filipe). Special marine forecasts (provided daily) are required for hurricane threats because of large coastal zones where there are fishing activities, hotels, and other tourist attractions.

Hurricane Fred and future vulnerability to anthropogenic climate change. The rapid intensification of Hurricane Fred from 28 to 31 August occurred when eastern Atlantic SSTs were up to 2°C above normal. Warmer SSTs due to anthropogenic climate change in the future may lead to rapid intensification in coastal zones when TC genesis occurs (Kafatos et al. 2006; Villarini and Vecchi 2013), along with a possible increase in TC frequency (Emanuel 2013). In addition, twenty-first-century anthropogenic climate change is expected to lead the thermal expansion of oceans, and the possible loss of ice sheets will raise the sea level (IPCC 2013), increasing the potential for damage along coastal zones in West Africa and Cape Verde in the presence of tropical disturbances. Countries in these zones must prepare for the eventuality of rising sea level through the building of sea walls and potentially moving vulnerable inhabitants away from coastal zones. Increasing populations in West Africa during the twenty-first century, especially in large urban coastal cities (Dakar, Banjul, Bissau, Nouakchott, Praia, Conakry, and their sprawling coastal suburban zones), are likely to be impacted by coastal storms and rising sea levels; solutions will be required to protect these populations.

ACKNOWLEDGMENTS. This work was supported by the Department of Meteorology at The Pennsylvania State University. Support for coauthor Chiao was provided by the NASA Office of Education's Minority University Research and Education Project (MUREP) Institutional Research Opportunity (MIRO) Contract NNX15AQ02A. We also thank the two reviewers for their useful comments for improving the manuscript.

REFERENCES

Beven, J. L., 2016: National Hurricane Center Tropical Cyclone Report: Hurricane Fred (AL062015). NOAA/NWS, 16 pp., www.nhc.noaa.gov/data/tcr/AL062015_Fred.pdf.

Braun, S. A., and Coauthors, 2013: NASA's Genesis and Rapid Intensification Processes (GRIP) field experiment. *Bull. Amer. Meteor. Soc.*, **94**, 345–363, https://doi.org/10.1175/BAMS-D-11-00232.1.

Carlson, T., and J. M. Prospero, 1972: The large-scale movement of Saharan air outbreaks over the northern equatorial Atlantic. *J. Appl. Meteor.*, **11**, 283–297,

https://doi.org/10.1175/1520-0450(1972)011<0283:TLSMOS>2.0.CO;2.

Chiao, S., and G. S. Jenkins, 2010: Numerical investigations on the formation of Tropical Storm Debby during NAMMA-06. *Wea. Forecasting*, **25**, 866–884, https://doi.org/10.1175/2010WAF2222313.1.

Emanuel, K. A. 2013. Downscaling CMIP5 climate models shows increased tropical cyclone activity over the 21st century. *Proc. Natl. Acad. Sci. USA*, **110**, 12 219–12 224, https://doi.org/10.1073/pnas.1301293110.

Evan, A. T., J. Dunion, J. A. A. K. Foley, K. Heidinger, and C. S. Velden, 2006: New evidence for a relationship between Atlantic tropical cyclone activity and African dust outbreaks. *Geophys. Res. Lett.*, **33**, L19813, https://doi.org/10.1029/2006GL026408.

Huffman, G. J., D. T. Bolvin, E. J. Nelkin, D. B. Wolff, R. F. Adler, G. Gu, Y. Hong, K. P. Bowman, and E .F. Stocker, 2007: The TRMM Multisatellite Precipitation Analysis (TMPA): Quasi-global, multiyear, combined-sensor precipitation estimates at fine scales. *J. Hydrometeor.*, **8**, 38–55, https://doi.org/10.1175/JHM560.1.

INE-CV, 2011: Censo 2010, Características Económicas da População, Praia. INE.

IPCC, 2007: *Climate Change 2007: The Physical Science Basis*. Cambridge University Press, 996 pp.

Janowiak, J. E., R. J. Joyce, and Y. Yarosh, 2001: A real-time global half-hourly pixel-resolution infrared dataset and its applications. *Bull. Amer. Meteor. Soc.*, **82**, 205–217, https://doi.org/10.1175/1520-0477(2001)082<0205:ARTGHH>2.3.CO;2.

Jenkins, G. S., A. S. Pratt, and A. Heymsfield, 2008: Possible linkages between Saharan dust and tropical cyclone rain band invigoration in the eastern Atlantic during NAMMA-06. *Geophys. Res. Lett.*, **35**, L08815, https://doi.org/10.1029/2008GL034072.

Kafatos, M., D. Sun, R. Gautam, Z. Boybeyi, R. Yang, and G. Cervone, 2006: Role of anomalous warm gulf waters in the intensification of Hurricane Katrina. *Geophys. Res. Lett.*, **33**, L17802, https://doi.org/10.1029/2006GL026623.

Koren, I., Y. J. Kaufman, D. Rosenfeld, L. A. Remer, and Y. Rudich, 2005: Aerosol invigoration and restructuring of Atlantic convective clouds. *Geophys. Res. Lett.*, **32**, L14828, https://doi.org/10.1029/2005GL023187.

Landsea, C., J. Franklin, and J. Beven, 2013: The revised Atlantic hurricane database (HURDAT2). NOAA, www.nhc.noaa.gov/data/#hurdat.

Montgomery, M. T., and Coauthors, 2012: The Pre-Depression Investigation Of Cloud-Systems in the Tropics (PREDICT) experiment: Scientific basis, new analysis tools, and some first results. *Bull. Amer. Meteor. Soc.*, **93**, 153–172, https://doi.org/10.1175/BAMS-D-11-00046.1.

Obasi, G. O. P., 1994: WMO's role in the international decade for natural disaster reduction. *Bull. Amer. Meteor. Soc.*, **75**, 1655–1661, https://doi.org/10.1175/1520-0477(1994)075<1655:WRITID>2.0.CO;2.

Rogers, R., and Coauthors, 2013: NOAA'S Hurricane Intensity Forecasting Experiment: A progress report. *Bull. Amer. Meteor. Soc.*, **94**, 859–882, https://doi.org/10.1175/BAMS-D-12-00089.1.

Rosenfeld, D., W. L. Woodley, A. Khain, W. R. Cotton, G. Carrió, I. Ginis, and J. H. Golden, 2012: Aerosol effects on microstructure and intensity of tropical cyclones. *Bull. Amer. Meteor. Soc.*, **93**, 987–1001, https://doi.org/10.1175/BAMS-D-11-00147.1.

Sall, S. M., and H. Sauvageot, 2005: Cyclogenesis off the African coast: The case of Cindy in August 1999. *Mon. Wea. Rev.*, **133**, 2803–2813, https://doi.org/10.1175/MWR3003.1.

Skamarock, W. C., and Coauthors, 2008: A description of the Advanced Research WRF version 3. NCAR Tech. Note NCAR/TN-475+STR, 113 pp., https://doi.org/10.5065/D68S4MVH.

Villarini, G., and G. A. Vecchi, 2013: Projected increases in North Atlantic tropical cyclone intensity from CMIP5 models. *J. Climate*, **26**, 3231–3240, https://doi.org/10.1175/JCLI-D-12-00441.1.

Zawislak, J., and E. J. Zipser, 2010: Observations of seven African easterly waves in the east Atlantic during 2006. *J. Atmos. Sci.*, **67**, 26–43, https://doi.org/10.1175/2009JAS3118.1.

Zipser, E. J., and Coauthors, 2009: The Saharan air layer and the fate of African easterly waves—NASA's AMMA field study of tropical cyclogenesis. *Bull. Amer. Meteor. Soc.*, **90**, 1137–1156, https://doi.org/10.1175/2009BAMS2728.1.